Cancer Cell
Article

The Crosstalk of mTOR/S6K1 and Hedgehog Pathways

Yan Wang,[1] Qingqing Ding,[1] Chia-Jui Yen,[1] Weiya Xia,[1] Julie G. Izzo,[2,3] Jing-Yu Lang,[1] Chia-Wei Li,[1] Jennifer L. Hsu,[1,8,14] Stephanie A. Miller,[1] Xuemei Wang,[4] Dung-Fang Lee,[1,9] Jung-Mao Hsu,[1,9] Longfei Huo,[1] Adam M. LaBaff,[1,9] Dongping Liu,[1] Tzu-Hsuan Huang,[1] Chien-Chen Lai,[7,10] Fuu-Jen Tsai,[6] Wei-Chao Chang,[8,11] Chung-Hsuan Chen,[11] Tsung-Teh Wu,[12] Navtej S. Buttar,[13] Kenneth K. Wang,[13] Yun Wu,[5] Huamin Wang,[5] Jaffer Ajani,[3] and Mien-Chie Hung[1,8,9,14,*]

[1]Department of Molecular and Cellular Oncology
[2]Department of Experimental Therapeutics
[3]Department of Gastrointestinal Medical Oncology
[4]Department of Biostatistics
[5]Department of Pathology
University of Texas, MD Anderson Cancer Center, Houston, TX 77030, USA
[6]Department of Medical Research
[7]Graduate Institute of Chinese Medical Science
[8]Center for Molecular Medicine and Graduate Institute of Cancer Biology
China Medical University, 40402 Taichung, Taiwan
[9]Graduate School of Biomedical Sciences, University of Texas, Houston, TX 77030, USA
[10]Institute of Molecular Biology, National Chung Hsing University, Taichung 402, Taiwan
[11]Genomics Research Center, Academia Sinica, Taipei 115, Taiwan
[12]Department of Anatomic Pathology
[13]Division of Gastroenterology and Hepatology
Mayo Clinic, Rochester, MN 55905, USA
[14]Asia University, Taichung 41354, Taiwan
*Correspondence: mhung@mdanderson.org
DOI 10.1016/j.ccr.2011.12.028

SUMMARY

Esophageal adenocarcinoma (EAC) is the most prevalent esophageal cancer type in the United States. The TNF-α/mTOR pathway is known to mediate the development of EAC. Additionally, aberrant activation of Gli1, downstream effector of the Hedgehog (HH) pathway, has been observed in EAC. In this study, we found that an activated mTOR/S6K1 pathway promotes Gli1 transcriptional activity and oncogenic function through S6K1-mediated Gli1 phosphorylation at Ser84, which releases Gli1 from its endogenous inhibitor, SuFu. Moreover, elimination of S6K1 activation by an mTOR pathway inhibitor enhances the killing effects of the HH pathway inhibitor. Together, our results established a crosstalk between the mTOR/S6K1 and HH pathways, which provides a mechanism for SMO-independent Gli1 activation and also a rationale for combination therapy for EAC.

INTRODUCTION

Esophageal adenocarcinoma (EAC) is one of the most aggressive cancers in the world, characterized by high mortality and poor prognosis (Jemal et al., 2009). In the United States, EAC has increased at a frequency of 5%–10% per year since the 1980s, making it the fastest growing malignancy (Jemal et al., 2009). Despite multidisciplinary therapeutic approaches, EAC remains a virulent disease with an overall five-year survival rate <20% (Hongo et al., 2009). It is very urgent to identify therapeutic targets for prevention and establish biomarkers useful for early detection of high-risk populations. Esophageal chronic

Significance

The Hedgehog pathway plays a crucial role in many types of cancers, and several chemicals targeting SMO, the key mediator of canonical Hedgehog pathway, are being tested in clinical trials for cancer therapy. Although these chemicals have shown potential efficacy, the development of resistance has been also observed. Our data demonstrate that mTOR/S6K1 directly activates Gli1 independent of SMO, which results in the resistance of tumor cells to inhibitors targeting SMO. However, an mTOR inhibitor could enhance the inhibitory effects of SMO inhibitors on the tumor cells. Therefore, the combination of the inhibitors against the mTOR/S6K1 and Hedgehog pathways may be more effective in cancer target therapy.

inflammation induced by gastro-esophageal reflux disease is an important factor contributing to EAC (Lambert and Hainaut, 2007a, 2007b), and some inflammation-related cytokines have been found to play pivotal roles in the development of EAC, especially tumor necrosis factor (TNF)-α (Eksteen et al., 2001).

Our previous work has shown that TNF-α activates the mTOR pathway through IKKβ to stimulate the development and progression of EAC (Yen et al., 2008). The mechanistic target of rapamycin (mTOR) is a serine/threonine protein kinase, and its activation leads to the phosphorylation of S6K1 and 4E-BP1 (Guertin and Sabatini, 2007). S6K1 is also a serine/threonine kinase, and its phosphorylation by mTOR activates its function to promote the mRNA translation of target genes (Guertin and Sabatini, 2007). For 4E-BP1, however, phosphorylation by mTOR inactivates its function and de-represses its inhibition on cap-dependent translation (Guertin and Sabatini, 2007). The mTOR pathway has been established pivotally to be involved in many aspects of molecular and cellular biology, including mRNA translation, ribosome biogenesis, cell growth and survival, nutrient metabolism, immunosuppression, and aging, as well as cancers (Guertin and Sabatini, 2007). Moreover, the mTOR pathway is activated by TNF-α to promote angiogenesis (Lee et al., 2007a), which facilitates the chronic inflammation-induced cancers, including breast cancers (Lee et al., 2007a) and esophageal cancers (EC; Hildebrandt et al., 2009; Yen et al., 2008).

The Hedgehog (HH) signal pathway is also considered to be crucially involved in the development of esophageal cancers because it is overactivated and correlated with lymph node metastasis (Katoh and Katoh, 2009a; Lee et al., 2009). The HH pathway was identified first in *Drosophila* as an important regulator for proper embryonic patterning and is highly conserved from *Drosophila* to mammals (Ingham and McMahon, 2001). Three HH ligands have been identified in mammals: Sonic Hedgehog (SHH), Indian Hedgehog (IHH), and Desert Hedgehog (DHH; Ng and Curran, 2011), which are secreted and initiate signaling in receiving cells by binding and inactivating the HH receptor Patched 1 (PTCH1). Inhibition of PTCH1 releases the G-coupled receptor-like signal transducer Smoothened (SMO). SMO then activates glioma-associated oncogenes (Gli) through blocking their inhibitory partner, suppressor of fused (SuFu; Ng and Curran, 2011). Gli proteins, including Gli1, 2, and 3, are zinc finger transcription factors. Activated Gli proteins translocate into the nucleus and stimulate the transcription of HH pathway target genes, including Gli1, PTCH1, and many survival-promoting molecules (Jiang and Hui, 2008; Ng and Curran, 2011). Besides being activated by HH ligands-PTCH1-SMO axis, also known as the canonical HH pathway (Jenkins, 2009), Gli proteins, mainly Gli1, have been reported to be activated by AKT (Katoh and Katoh, 2009b; Stecca et al., 2007), MAPK/ERK (Seto et al., 2009), and KRAS (Nolan-Stevaux et al., 2009) in HH ligands-PTCH1-SMO axis-independent or SMO-independent manner (Ng and Curran, 2011). Although the canonical pathway has been well established, how Gli1 is regulated in a SMO-independent manner is still a puzzle.

Although both mTOR and HH pathways have been considered as drug targets in gastrointestinal (GI) cancer, including esophageal cancers (Wiedmann and Caca, 2005), the correlation between the two pathways has not been yet reported. Additionally, whether there is a relationship between TNF-α and HH pathway in EAC is also not clear. Therefore, in this work, we explored whether the TNF-α/mTOR pathway is involved in the activation of the HH pathway in EAC.

RESULTS

TNF-α Promotes Gli1 Activity through the mTOR Pathway

Because Gli protein activity is a useful readout for the HH pathway (Jiang and Hui, 2008), we employed a Gli-dependent luciferase reporter system (Sasaki et al., 1997) to evaluate the influence of TNF-α on the HH pathway in three EAC cell lines: BE3, SKGT-4, and OE33 (Boonstra et al., 2010). We observed that TNF-α increases the expression of the reporter (Figure 1A) and the mRNA levels of four Gli target genes (Figure 1B). Therefore, TNF-α can activate the HH pathway in the EAC cells. Then, we compared the activity of HH pathway in EAC cells stimulated by SHH or TNF-α. We found that there is constitutive activation of HH pathway in EAC cell lines, which can be inhibited by SMO inhibitors, cyclopamine and GDC-0449 (Scales and de Sauvage, 2009). Both SHH and TNF-α increased the activity of HH pathway in EAC cells with higher intensity from SHH (Figure S1A available online).

To investigate whether TNF-α induces Gli activity through SMO-dependent HH pathway, we pretreated the EAC cells with cyclopamine followed by TNF-α. Interestingly, cyclopamine did not affect the TNF-α-induced Gli activity (Figure 1C). Similarly, knock-down of SMO did not inhibit the TNF-α-induced Gli activity (Figure S1B). Therefore, TNF-α activates Gli function in a SMO-independent manner. To determine whether the mTOR pathway is involved in the regulation of Gli function by TNF-α, we used rapamycin and WYE-354 to block the mTOR pathway (Richard et al., 2010). Surprisingly, both compounds impaired TNF-α-stimulated Gli activation (Figures 1C and S1C). Therefore, TNF-α-stimulated Gli activation might require the activation of mTOR pathway. To further evaluate this possibility, we overexpressed wild-type mTOR or a rapamycin-resistant mTOR (mTORS2035T; Brown et al., 1995) in EAC cells followed by treatment of TNF-α alone or plus rapamycin. Western blot results confirmed that rapamycin blocked activation of mTOR pathway in mTOR-overexpressed cells but not in mTORS2035T-overexpressed cells (Figure S1D). Consistently, rapamycin suppressed the TNF-α-stimulated Gli reporter expression in mTOR-transfected EAC cells but barely had effect on mTORS2035T-transfected EAC cells (Figure 1F). Collectively, these results suggest that TNF-α activates Gli proteins through mTOR pathway.

Although Gli1, Gli2, and Gli3 all can regulate the expression of the Gli reporter (Jiang and Hui, 2008; Ng and Curran, 2011), only Gli1 knock-down impaired the TNF-α-stimulated expression of Gli reporter (Figure S1E), which suggests that TNF-α selectively activated Gli1. Consistently, TNF-α treatment rapidly induced Gli1 nuclear accumulation without obvious changes in the total protein level of Gli1 (Figure 1D, top panel). Rapamycin (Figure 1D, middle panel), but not cyclopamine (Figure 1D, bottom panel), blocked TNF-α-induced Gli1 nuclear accumulation, which was further supported by the immunofluorescence staining (Figures 1E, S1F, and S1G). Therefore, TNF-α promotes Gli1 nuclear localization and activation through the mTOR pathway.

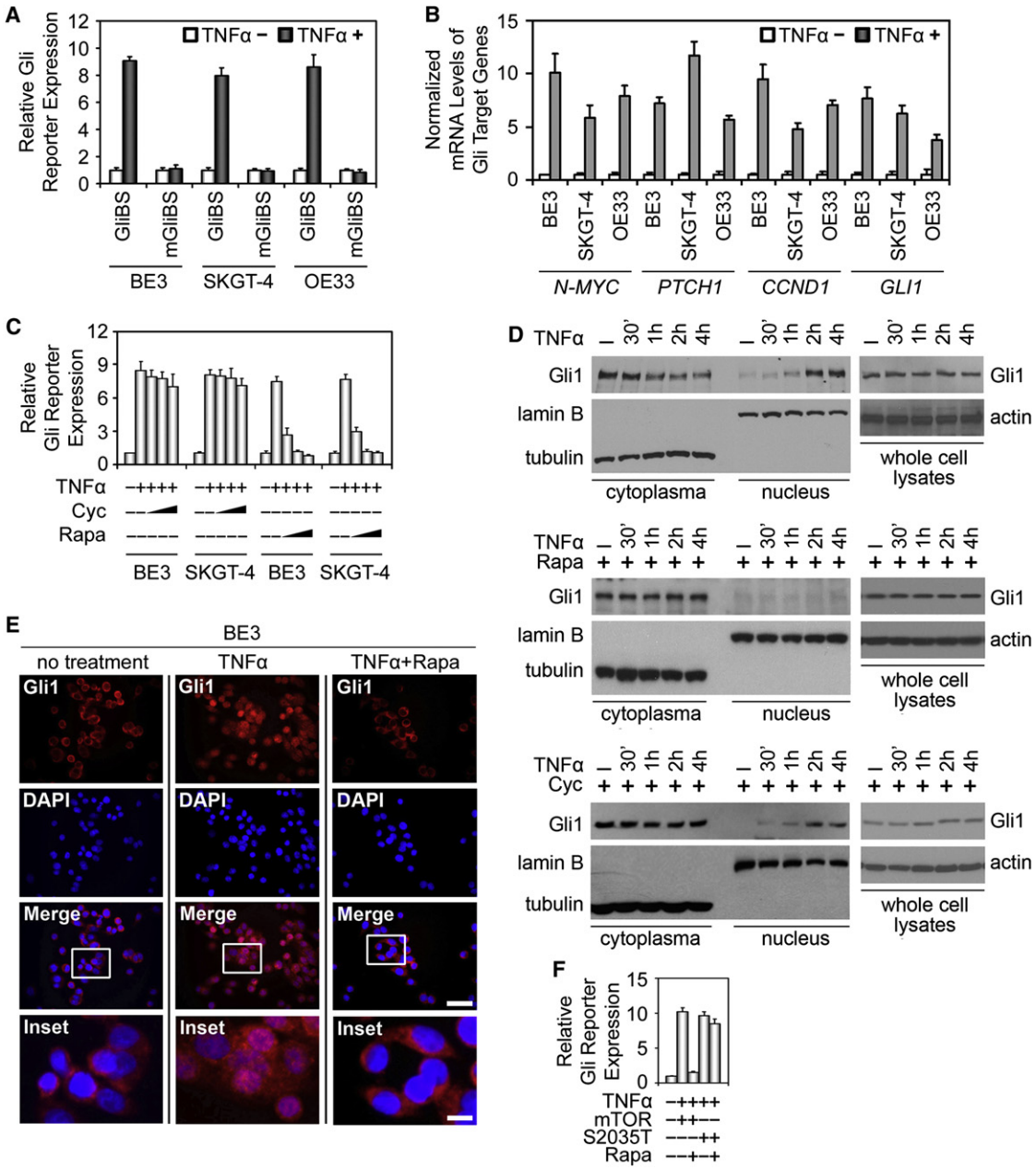

Figure 1. TNF-α Regulates Gli1 Transcriptional Activity

(A) Luciferase assay for Gli transcriptional activity in esophageal adenocarcinoma (EAC) cell lines with or without TNF-α (5 ng/ml) stimulation. The EAC cells were transfected using GliBS-Lucferase or mGliBS-Luciferase with CMV-Renilla at a 10:1 ratio, serum-starved overnight, and then treated with TNF-α for 24 hr. GliBS is Gli-responsive reporter, and mGliBS is Gli-unresponsive reporter. Error bars represent SD (n = 5).

(B) The mRNA levels of Gli1 target genes in the EAC cell lines with or without TNF-α (5 ng/ml) stimulation were examined by real-time PCR and normalized to the mRNA level of *ACTIN*. Error bars represent SD (n = 4).

(C) EAC cells were cotreated with TNF-α (5 ng/ml) and cyclopamine (Cyc; 0.5, 1, and 5 μM) or TNF-α (5 ng/ml) and rapamycin (Rapa; 10, 50, and 100 nM) for 24 hr and then subjected to luciferase assay. Error bars represent SD (n = 5 for cyclopamine treatment and n = 4 for rapamycin treatment).

(D) BE3 cells were treated with TNF-α (5 ng/ml) alone (top panel) or cotreated with TNF-α and rapamycin (50 nM, middle panel) or cyclopamine (1 μM, bottom panel) for indicated time course. Then, the cells were lysed for cell fractionation followed by western blotting. Lamin B and tubulin were used as markers for the nucleus and the cytoplasm, respectively.

(E) Immunofluorescent analysis of Gli1 in BE3 cells treated with TNF-α (5 ng/ml) alone or cotreated with TNF-α and rapamycin (50 nM). Scale bar = 100 μm for original picture and 25 μm for inset. Dapi was used to stain nuclei.

(F) Luciferase assay for Gli reporter using BE3 cells transfected with wild-type mTOR or rapamycin-resistant mTOR (mTORS2035T) followed by treatment of TNF-α alone or in combination with rapamycin (50 nM). Error bars represent SD (n = 4).

See also Figure S1.

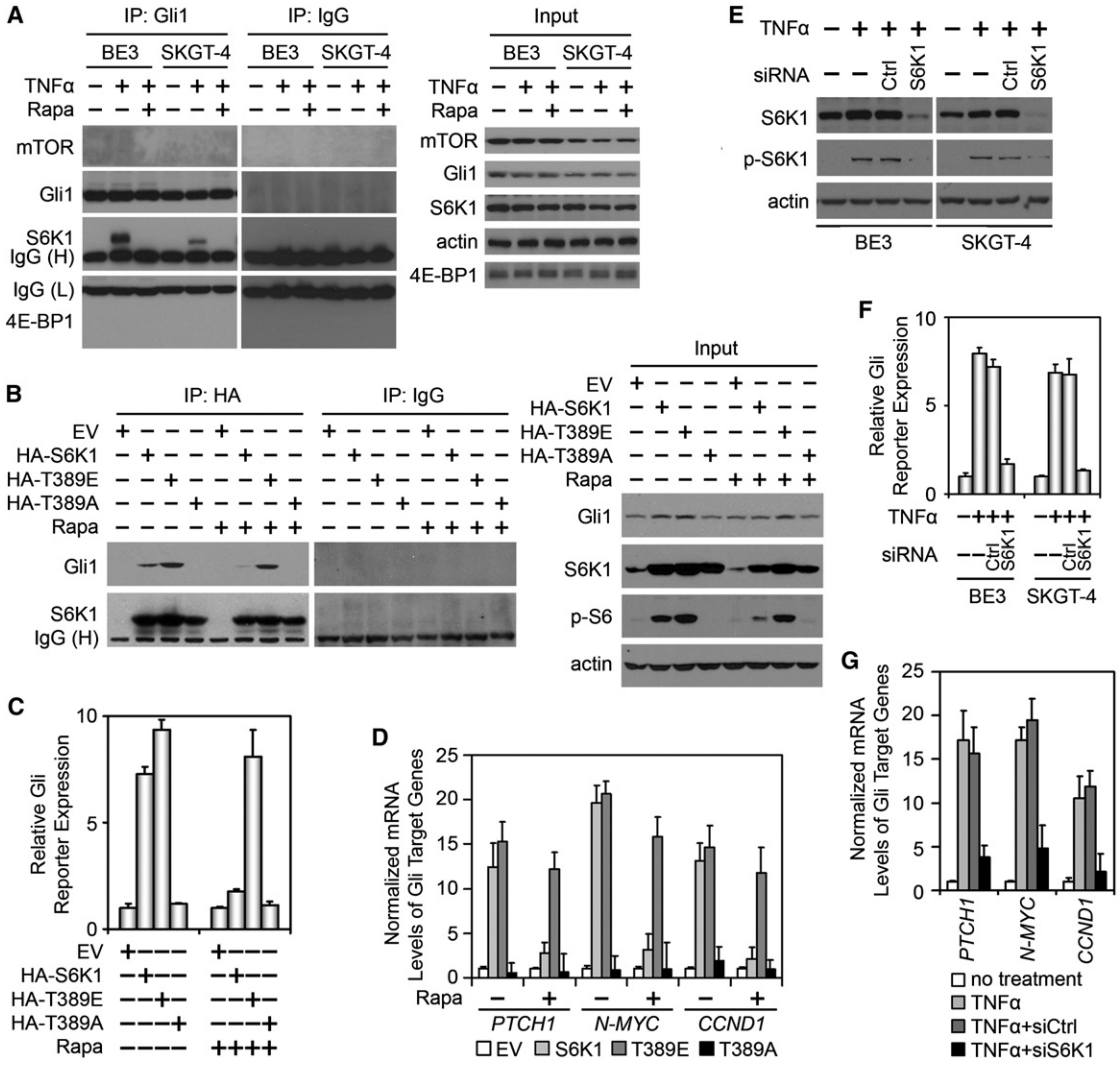

Figure 2. S6K1 Mediates the Regulation of Gli1 by TNF-α

(A) BE3 or SKGT4 cells were treated with TNF-α (5 ng/ml) alone or cotreated with TNF-α and rapamycin (50 nM) for 6 hr, and then the cells were lysed and subjected to IP-western blot assay to examine the interactions between mTOR pathway components with Gli1.

(B) BE3 cells were transiently transfected with HA-tagged wild-type S6K1 (HA-S6K1), constitutively activated S6K1T389E (HA-T389E), function-loss S6K1T389A (HA-T389A), or empty vector (EV). After 24 hr of the transfection, the cells were treated with or without rapamycin (100 nM) for additional 6 hr followed by lysis and IP-western assay to test the interaction between S6K1 variants and Gli1. Phosphorylated S6 (p-S6) was used as marker for S6K1 activation.

(C) BE3 cells were transiently transfected with Gli-firefly and CMV-renilla reporters in combination with HA-S6K1, HA-T389E, HA-T389A, or EV. After 24 hr of the transfection, the cells were treated with or without rapamycin (100 nM) for additional 24 hr followed by luciferase assay to measure the expression of Gli reporter. Error bars represent SD (n = 3).

(D) The mRNA levels of Gli1 target genes in the BE3 cells transiently transfected with HA-S6K1, HA-T389E, HA-T389A, or EV followed by treatment with or without rapamycin (100 nM) measured via real-time PCR. The mRNA levels of Gli1 target genes were normalized to the mRNA level of *ACTIN*. Error bars represent SD (n = 3).

(E) Western blot analysis using the EAC cells transfected with control siRNA (Ctrl) or siRNA targeting S6K1 followed by TNF-α treatment.

(F) EAC cells were transiently transfected with control siRNA (Ctrl) or siRNA targeting S6K1. After 48 hr of the transfection, the cells were further transfected with Gli-firefly and CMV-renilla reporters with or without TNF-α for additional 24 hr followed by luciferase assay. Error bars represent SD (n = 3).

(G) BE3 cells were transiently transfected with control siRNA (Ctrl) or siRNA targeting S6K1 followed by treatment with TNF-α or only treated with TNF-α. The mRNA levels of Gli1 target genes in these cells were measured respectively through real-time PCR and normalized to the mRNA level of *ACTIN*. Error bars represent SD (n = 3).

See also Figure S2.

S6K1 Mediates the Regulation of Gli1 by TNF-α

To investigate how the mTOR pathway activates Gli1 activity, we examined whether Gli1 interacts with the components of mTOR pathway. Without TNF-α, no interactions were found between Gli1 and mTOR pathway components; with TNF-α stimulation, however, a clear interaction was observed between Gli1 and S6K1 but not between Gli1 and mTOR or 4EB-P1 (Figures 2A and S2A). Since Gli1 function is inhibited by SuFu, we also

examined whether there are any interactions between the mTOR pathway components and SuFu. Unlike Gli1, SuFu did not interact with mTOR, S6K1, or 4EB-P1, regardless of TNF-α treatment (Figure S2B). Moreover, neither Gli2 nor Gli3 bound to mTOR, S6K1, or 4EB-P1 (Figures S2C and S2D). Taken together, the mTOR pathway might regulate Gli1 via S6K1.

Because S6K1 bound to Gli1 only under TNF-α stimulation, we hypothesized that S6K1 might need to be activated to interact with Gli1. To address this point, wild-type S6K1, constitutively activated S6K1 (S6K1T389E), or function-loss S6K1 (S6K1T389A; Holz et al., 2005) was transfected into the BE3 cells. S6K1 and S6K1T389E increased S6K1 activity, as indicated by increase of phosphorylation of S6, a substrate of S6K1 (Figure 2B). Rapamycin could inhibit the activity of S6K1, but not S6K1T389E (Figure 2B; Holz et al., 2005). Both S6K1 and S6K1T389E interacted with Gli1, and rapamycin effectively inhibited the interaction between S6K1 and Gli1, but not between S6K1T389E and Gli1 (Figure 2B). In addition, ectopic expression of S6K1T389A did not interact with Gli1 (Figure 2B). Furthermore, ectopic expression of S6K1 or S6K1T389E, but not S6K1T389A, increased the expression of Gli reporter and Gli1 target genes (Figures 2C and 2D). Rapamycin blocked the effects of S6K1 on Gli reporter expression but did not affect that of S6K1T389E (Figures 2C and 2D). Thus, only the activated S6K1 formed complex with Gli1 and enhanced its activity.

To investigate whether S6K1 mediates the regulation of Gli1 by TNF-α, we knocked down S6K1 (Figure 2E) and tested the regulation of Gli1 by TNF-α. The results indicated that the TNF-α-stimulated Gli1 activity and expression of Gli target genes were impeded by S6K1 knock-down (Figures 2F and 2G). Additionally, the inhibition of TNF-α-stimulated Gli1 activation by siRNA, which targeted 3′UTR region of S6K1 mRNA, was rescued by expression of an exogenous S6K1 lacking of 3′UTRs but not by expression of exogenous S6K1T389A or a kinase-dead S6K1 (S6K1 K100R; Holz et al., 2005; Figures S2E and S2F). Therefore, activated S6K1 is required for the regulation of Gli1 by the TNF-α/mTOR pathway.

Gli1 Is Phosphorylated by S6K1 and Required for TNF-α/mTOR/S6K1-Mediated Cell Proliferation

Since S6K1 is a serine/threonine kinase, we asked whether S6K1 regulates Gli1 through phosphorylation. Indeed, serine/threonine phosphorylation of Gli1 was observed with the ectopic expression of S6K1 or S6K1T389E (Figure 3A) but not of S6K1T389A or S6K1K100R (Figure 3A). Furthermore, an in vitro kinase assay showed that only the Gli1 fragment containing 1-500aa, Gli1F1, was phosphorylated by S6K1 but not by S6K1K100R (Figure 3B). The phosphorylation level of Gli1F1 fragment is comparable to that of S6, suggesting that Gli1 was a substrate of S6K1 in vitro. We identified 79-KKRALS-84 (Figure S3A), which is highly conserved from fruit fly to human (Figure 3C), as one potential S6K1-recognizing motif (K/RxRxxS/T) in Gli1F1. When Ser84 was mutated to alanine (Gli1S84A), phosphorylation of Gli1 by S6K1 disappeared (Figure 3D), suggesting that the Ser84 in Gli1 is the site phosphorylated by S6K1 in vitro.

To assess whether this phosphorylation occurs in vivo, we performed mass spectrometric analysis using BE3 cells treated with TNF-α alone or TNF-α and rapamycin. The results showed that the phosphorylation of Gli1 Ser84 was detected in cells treated with TNF-α but not in cells treated with rapamycin and TNF-α (Figure S3B). Thus, the activation of the mTOR/S6K1 pathway contributes to the phosphorylation of Gli1 Ser84. To further investigate endogenous Gli1 phosphorylation by TNF-α or S6K1, we developed a mouse polyclonal antibody that specifically recognizes phosphorylated Ser84 of Gli1 (p-Gli1S84). This antibody recognized TNF-α-stimulated flag-Gli1 but not without TNF-α or flag-Gli1S84A, regardless of TNF-α treatment (Figure S3C). Using this antibody, we found that TNF-α stimulation or S6K1 ectopic expression effectively induced Gli1 Ser84 phosphorylation (Figure 3E), which was diminished by the addition of rapamycin (Figure 3E). Notably, phosphorylated Gli1 was observed mainly in the nucleus (Figure 3F), which implied that the phosphorylated Gli1 might be functionally activated. The TNF-α-stimulated phosphorylation of Gli1 was largely inhibited when S6K1 was knocked down by siRNA targeting 3′UTR but could be effectively rescued by exogenous S6K1 (Figure 3G). Together, the results suggest that S6K1 mediates the regulation of Gli1 by the TNF-α/mTOR pathway through phosphorylating Gli1 at Ser84.

We also investigated if Gli1 activation is required for the effects of the TNF-α/mTOR/S6K1 pathway on cellular oncogenecity. We detected clear signals of p-Gli1S84 in BE3 and OE33 (Figure S3D), and knock-down of Gli1 impaired the TNF-α-stimulated, as well as S6K1 ectopic, expression-increased cell viability, proliferation, and invasion (Figures S3E and S3F). Thus, the activation of Gli1 by S6K1 is functionally involved in the TNF-α/mTOR pathway.

Besides TNF-α, we tested whether other mTOR pathway stimulators led to Gli1 phosphorylation. Amino acids also induced the phosphorylation of Gli1S84 in BE3 cells (Figure S3H). Furthermore, the phosphorylation of Gli1S84 in $TSC2^{-/-}$ MEFs, which has constitutive activation of the mTOR pathway and S6K1, is increased compared with $TSC^{+/+}$ MEFs (Figure S3G). Therefore, the activation of the mTOR pathway is an important stimulator for Gli1 phosphorylation in both cancer and noncancerous cells.

The mTOR pathway includes two complexes. The first is mTOR complex 1 (mTORC1), which requires raptor and activates S6K1, and the second is mTORC2, which requires rictor and activates AKT (Zoncu et al., 2011). Rapamycin and WYE-354 inhibit both mTORC1 and mTORC2 (Richard et al., 2010). Therefore, we asked whether mTORC2 also regulates Gli1 phosphorylation. Although knock-down of mTOR or raptor impaired the TNF-α-mediated Gli1 phosphorylation and activation, knock-down of rictor did not (Figures 3H and S3I), indicating that only mTORC1 plays a role in the regulation of Gli1.

Gli1 Phosphorylation by S6K1 Augments the Gli1 Function and Inhibits SuFu Binding

Since Gli1 is regulated by S6K1 in EAC cells, we wanted to know if Gli1 is required for EAC transformation. We established BE3 stable clones with Gli1 knock-down (Figure 4A), and as expected, transcription of Gli1 target genes decreased with Gli1 knock-down (Figure 4B). Moreover, Gli1 knock-down also decreased cell proliferation (Figures 4C and 4D), migration (Figure S4A), invasion (Figure S4B), and anchorage-independent growth ability (Figure S4C). Thus, Gli1 is functionally required for EAC cells. Then, to understand the effects of Ser84

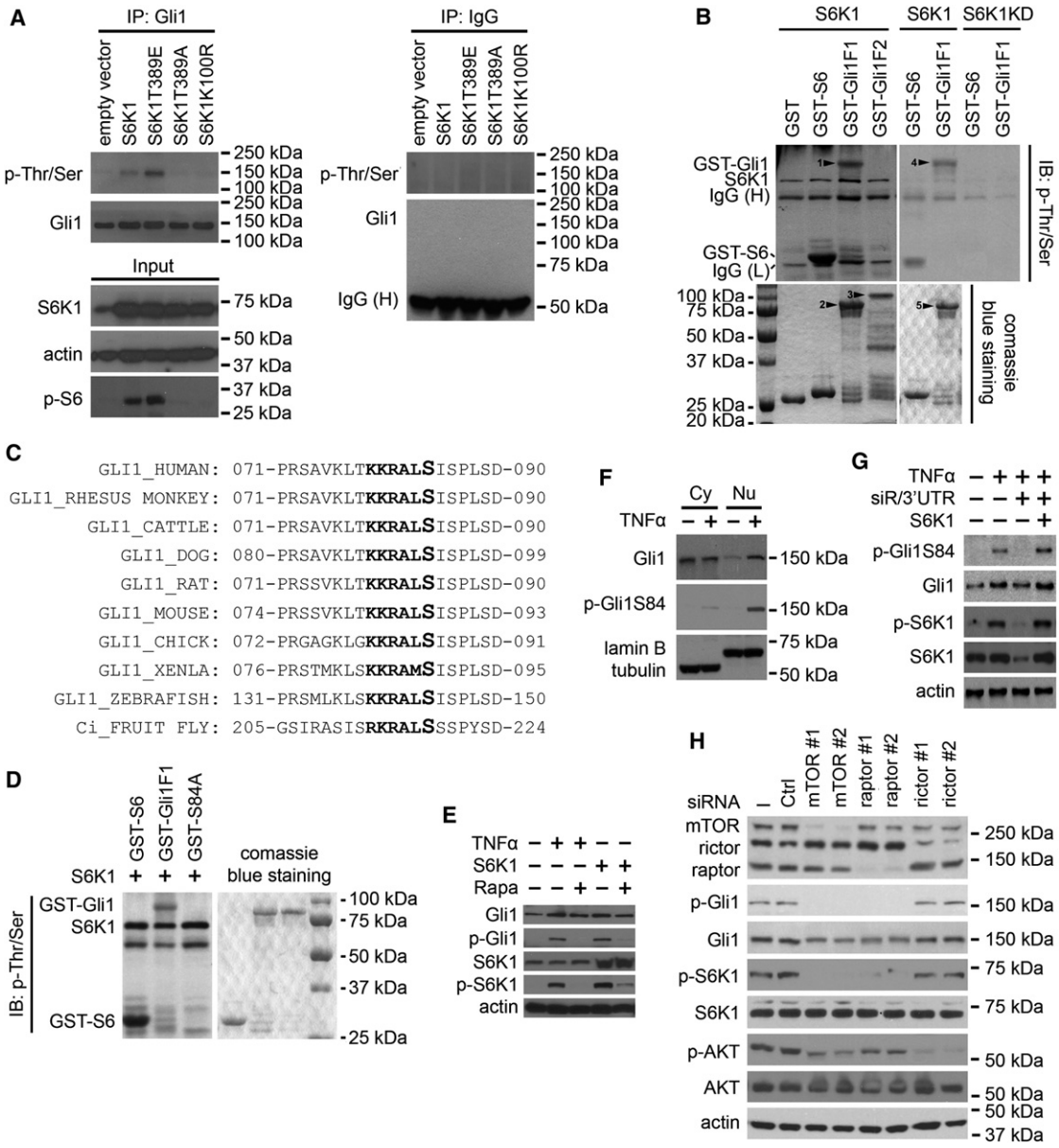

Figure 3. S6K1 Phosphorylates Gli1 at Ser84

(A) The empty vector, wild-type S6K1, S6K1T389E, S6K1T389A, or kinase-dead S6K1 (S6K1K100R) was introduced into the BE3 cells, and endogenous Gli1 was immunoprecipitated for western blot analysis. The phosphorylation was examined using anti-phospho-serine/threonine antibody.

(B) In vitro kinase assay using purified Gli1 fragment, containing 1–500 amino acids (Gli1F1), or Gli1F2, containing amino acid 501 to the end, plus purified wild-type S6K1 kinase or kinase-dead S6K1 (S6K1KD). Arrowheads 1 and 4 show phosphorylated Gli1F1 detected using anti-phospho-serine/threonine antibody; arrowheads 2 and 5 are purified Gli1F1 protein; and arrowhead 3 is purified Gli1F2 protein. The phosphorylation of S6 acts as a positive control.

(C) The S6K1 recognizing motif in Gli1 from fruit fly to human.

(D) In vitro kinase assay using purified Gli1F1 or Gli1F1 with the alanine substitution of serine 84 (S84A) plus purified S6K1.

(E) With the absence or presence of rapamycin (100 nM), BE3 cells were transiently transfected with S6K1 expression plasmid or treated with TNF-α (5 ng/ml). The phosphorylation of Gli1S84 was detected using phosphor-Gli1S84-specific antibody in western blot analysis.

(F) BE3 cells were treated with TNF-α (5 ng/ml) for 6 hr, and then the cells were lysed for cell fractionation and subsequent western blot analysis. The phosphorylation of Gli1S84 was detected using phosphor-Gli1S84-specific antibody. Lamin B and tubulin were used as markers for the nucleus and cytoplasm, respectively.

(G) BE3 cells were treated with TNF-α alone, or TNF-α plus siRNA targeting S6K1 mRNA 3′UTR with or without transfection of S6K1 expression plasmid, and then the cells were lysed for western blot analysis.

(H) Western blot analysis of BE3 cells transfected with control siRNA, or siRNA targeting mTOR, raptor, and rictor, respectively.

See also Figure S3.

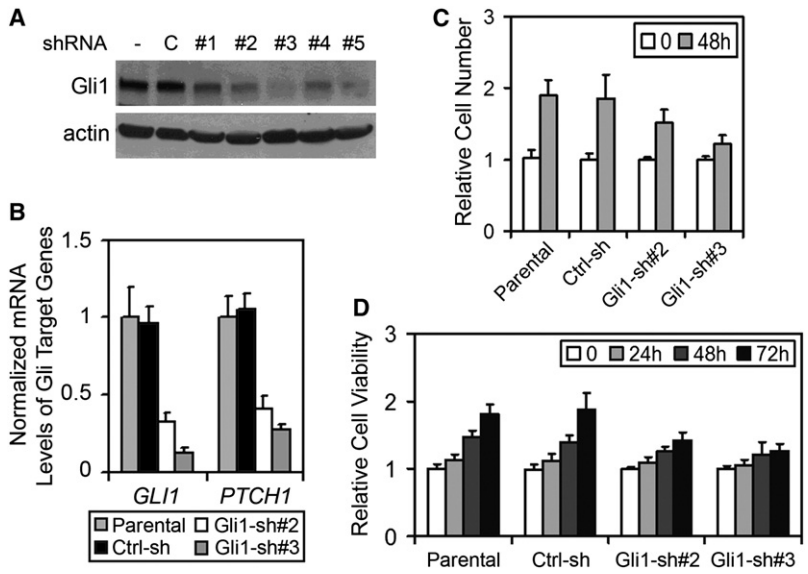

Figure 4. Knock-Down of Gli1 in EAC Cells Decreases Cell Proliferation, Migration, Invasion, and Colony Formation

(A) The BE3 stable clones with Gli1 knock-down. C, non-silencing control shRNA; #1–5, five different Gli1 shRNAs.

(B) The mRNA levels of Gli1 target genes in the BE3 stable clones with Gli1 knock-down measured via real-time PCR and normalized to the mRNA level of *ACTIN*. Error bars represent SD (n = 3).

(C) Cell counting analysis of the BE3 stable clones with Gli1 knock-down. All cells were counted, and then 1×10^5 cells were seeded in 10 cm dishes. Error bars represent SD (n = 3).

(D) MTT (3-(4,5-Dimethylthiazol-2-yl)-2,5-diphenyltetrazolium bromide) assay of the BE3 stable clones with Gli1 knock-down. All cells were counted, and then 3,000 cells were seeded in each well of a 96-well plate. Error bars represent SD (n = 3).

See also Figure S4.

phosphorylation on Gli1 function, we generated stable clones of BE3 cells expressing wild-type Gli1 (BE3/Gli1), Gli1S84A (BE3/S84A), Gli1S84E (BE3/S84E), or with the empty vector (BE3/EV). For Gli1S84E, Ser84 was mutated into glutamine to mimic constitutive phosphorylation of Gli1 at Ser84. We found that with similar Gli1 expression levels, BE3/S84E bore much higher Gli1 transcriptional activity and mRNA levels of Gli1 target genes among all the stable clones (Figures 5A and 5B). Consistently, the immunofluorescence staining showed that the level of nuclear Gli1 was much higher in BE3/S84E cells than BE3/Gli1 and BE3/S84A (Figure 5C). To further confirm that the functional difference was due to the mutations of Gli1, we treated these cells with TNF-α alone or together with rapamycin and found that TNF-α markedly induced the Gli1 transcriptional activity in BE3/Gli1, which was inhibited by cotreatment of rapamycin, but did not affect the Gli1 activity in BE3/S84E and BE3/S84A (Figure S5A). The results suggest that both S84E and S84A mutants were insensitive to TNF-α stimulation. The immunofluorescence staining further showed that TNF-α could enhance Gli1 nuclear localization in BE3/Gli1 cells but not in BE3/S84E or BE3/S84A cells (Figures 5C and S5B). Moreover, the p-Gli1S84 level also increased with TNF-α stimulation but gradually decreased with increased rapamycin dose (Figure S5C). Taken together, TNF-α-stimulated S84 phosphorylation increases Gli1 nuclear localization and transcriptional activity, and S84E and S84A mutants, mimicking phosphorylated and nonphosphorylated Gli1, respectively, are no longer sensitive to TNF-α.

Many reports have described Gli1 as an oncogene (Jiang and Hui, 2008; Ng and Curran, 2011); hence, we investigated the relationship between Gli1 phosphorylation and its tumorigenic functions. Gli1S84E and wild-type Gli1 but not Gli1S84A increased cell proliferation (Figure S5D). The Gli1S84E stable clones also exhibited the highest level of colony formation activity in soft-agar assay (Figure S5E). BE3/S84E exhibited much higher invasive ability than BE3/Gli1 and BE3/S84A (Figure S5F). These results support that the phosphorylation of Gli1 at Ser84 enhances Gli1 function. To further address why the wild-type Gli1 did not show strong biological activities in Figures S5E–S5F, we treated the BE3/Gli1 stable clone with TNF-α. Interestingly, we observed increased cell proliferation, anchorage-independent growth, and invasion (Figures S5G–S5I). Notably, TNF-α did not affect the BE3/S84E and BE3/S84A stable cells (Figures S5G–S5I). Therefore, the TNF-α/mTOR pathway promotes Gli1 function mostly via the Gli1 Ser84 phosphorylation. Furthermore, we tested the tumorigenicity of these cells by subcutaneously injecting them into the nude mice. Consistent with our in vitro data, BE3/S84E had the strongest tumorigenicity among all stable cells. Whereas BE3/Gli1 also led to tumor growth in nude mice, the tumors were smaller than those from BE3/S84E. BE3/EV and BE3/S84A induced only small tumor formation (Figures 5D and S5J). All these data indicated that Gli1 Ser84 is a key site for Gli1 activity, and its phosphorylation by S6K1 enhances Gli1 function as an oncogene.

It has been reported that without HH ligand stimulation, Gli1 function is inhibited by SuFu (Cheng and Yue, 2008). We therefore investigated whether Gli1 Ser84 phosphorylation affects its binding with SuFu. A co-immunoprecipitation experiment showed that the interaction between SuFu and Gli1 was markedly decreased in BE3/S84E compared with BE3/Gli1 and BE3/S84A (Figure 5E), which suggested that the Ser84 phosphorylation in Gli1 possibly reduced its binding to SuFu. Similarly, SuFu strongly interacted with exogenous Gli1WT and Gli1S84A but only weakly with Gli1S84E (Figure S5K). Furthermore, both TNF-α treatment and S6K1 ectopic expression decreased the binding between SuFu and Gli1, which was fully reversed by rapamycin administration (Figure 5F). Taken together, TNF-α/S6K1-induced phosphorylation of Gli1Ser84 attenuates SuFu-mediated Gli1 inhibition.

S6K1 and Gli1 Are Positively Correlated in Human Tumor Tissues

To investigate the significance of Gli1 regulation by S6K1 in human EAC tissues, we first validated suitability by immunohistochemistry (IHC) of the anti-Gli1 antibody that we would use,

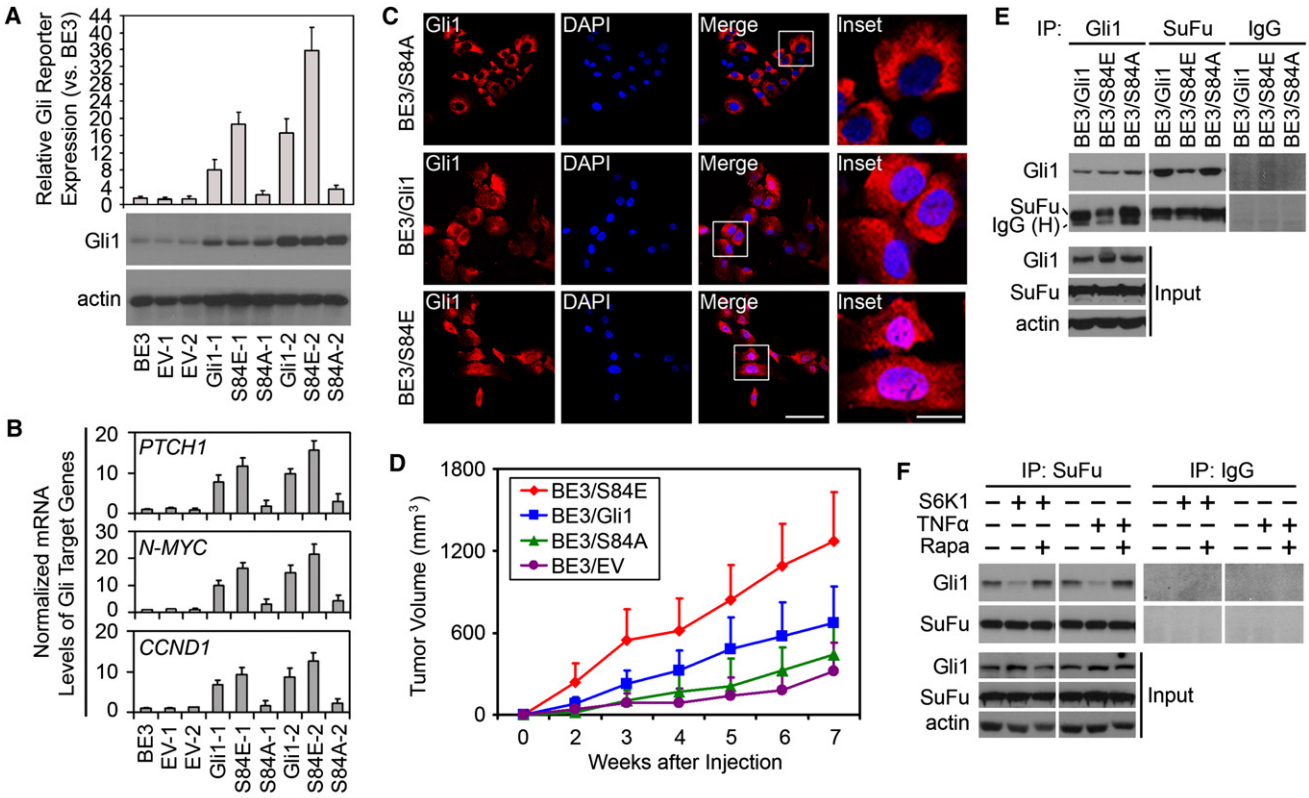

Figure 5. Functional Effects of S6K1-mediated Gli1 Phosphorylation

(A) Gli1 protein levels and Gli reporter activity in BE3 parental cells and the stable clones established from BE3 parental cells. EV, empty vector; S84A, alanine mutant of Gli1 Ser84; S84E, glutamine mutant of Gli1 Ser84. Error bars represent SD (n = 3).

(B) The mRNA levels of the Gli1 target genes in BE3 parental cells and stable clones were examined through real-time PCR and normalized to the level of *ACTIN*. Error bars represent SD (n = 3).

(C) Immunofluorescent analysis of Gli1 in the BE3 stable clones. Scale bar = 100 μm for original picture and 25 μm for inset. DAPI was used to stain nuclei.

(D) In vivo tumorigenesis assay of the stable clones in nude mice. BE3 stable cells (1×10^5) were subcutaneously injected into the right flank of nude mice, and tumor volume was measured and calculated using the formula $l \times w^2$, where l is the longest diameter and w is the shortest diameter. Error bars represent SD (n = 5).

(E) Interactions between Gli1 and SuFu in the stable clones through IP-western analysis.

(F) Endogenous interactions between Gli1 and SuFu in BE3 cells with the treatment of TNF-α (5 ng/ml) or ectopic expression of S6K1 with or without rapamycin (50 nM).

See also Figure S5.

even though it had been used for IHC before (Di Marcotullio et al., 2006; Fukaya et al., 2006). Consistent with a previous report (Kolterud et al., 2009), the staining in normal mouse colon tissues using this antibody showed that the Gli1 signal (brown color indicated by the arrows) is mainly localized in stromal cells (Figure S6A, left panel). Furthermore, western blot analysis of EAC cell lines using this antibody showed a single band at about 150 kDa (Figure S6B), which is consistent with the Gli1 molecular weight. When Gli1 was knocked down, the signal detected by the antibody concomitantly decreased compared with that from the parental or control siRNA-transfected cells (Figure S6C). This antibody was raised against amino acids 781–1080 of Gli1, and the Gli1 staining was completely blocked by a GST-Gli1 fragment containing amino acids 501–1160 but not by the fragment containing amino acids 1–500 (Figure S6D). Therefore, this anti-Gli1 antibody is applicable for IHC experiment.

We then evaluated the levels of Gli1 and p-S6K1 in 107 EAC tissue specimens by IHC (Figures 6A and 6B). Expression of both proteins was found in most cases. Eighty out of the 107 for p-S6K1 (74.8%) and 87 of the 107 (81.3%) for Gli1 were positive (Figure 6A), and there was a strong correlation between the levels of p-S6K1 and Gli1 (Figure 6C). We also collected 15 samples from rat Barrett's esophagus models (Yen et al., 2008) and found that there were no p-S6K1 or Gli1 signals in normal esophageal squamous cells but observed strong signals of both p-S6K1 and Gli1 in three of five BE and three of five EAC tissue samples (Figure S6E). Together, these data further support the notion that the activation of mTOR/S6K1 and Gli1 pathways is involved in the transformation of esophagus. To ensure the Gli1S84 phosphorylation also exists in human EAC tumor tissues, we first tested the applicability of the anti-p-Gli1S84 antibody for IHC. We found that the staining of p-Gli1 could be blocked by phosphorylated Gli1 peptide used for

A

protein	n	negative	positive			
		0%	>0-10%	>10-25%	>25-50%	>50%
p-S6K1 (T389)	107	27 (25%)	31 (29%)	15 (14%)	21 (20%)	13 (12%)
Gli1	107	20 (19%)	18 (17%)	9 (8%)	31 (29%)	29 (27%)

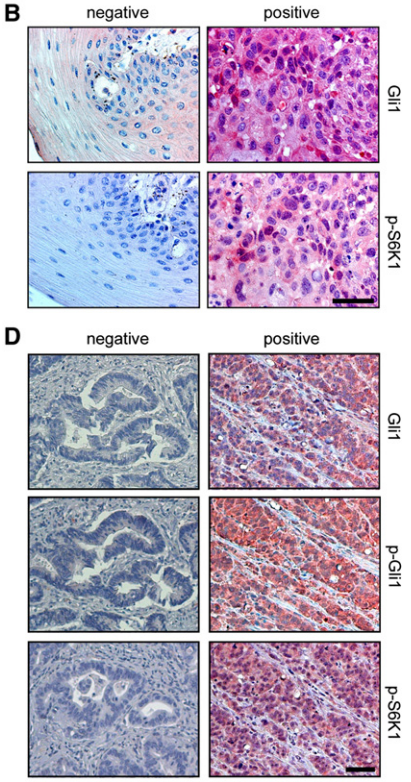

C

		Gli1		total
		negative	positive	
p-S6K1	negative	12	15	27
	positive	8	72	80
total		20	87	107
p = 0.0002				

E

		Gli1		total
		negative	positive	
p-S6K1	negative	15	15	30
	positive	8	32	40
total		23	47	70
p = 0.0108				

F

		p-Gli1		total
		negative	positive	
p-S6K1	negative	23	7	30
	positive	12	28	40
total		35	35	70
p = 0.0002				

G

$Gli1^+$ tissues		p-Gli1		total
		negative	positive	
p-S6K1	negative	8	7	15
	positive	4	28	32
total		12	35	47
p = 0.0093				

Figure 6. Correlations between p-S6K1T389 and Gli1 or p-Gli1S84 in EAC

(A) Statistic analysis of immunohistochemistry (IHC) staining of Gli1 and p-S6K1 from human EAC tissues.

(B) Representative IHC staining results for Gli1 and p-S6K1 in human EAC tissues. Scale bar = 50 μm.

(C) Statistic analysis for Gli1 and p-S6K1 correlation from the IHC staining results in human EAC tissues.

(D) Representative IHC staining results for p-Gli1 or p-S6K1 in human EAC tissue microarray. Scale bar = 50 μm.

(E) Statistic analysis for Gli1 and p-S6K1 correlation from the IHC staining results in human EAC tissue microarray.

(F) Statistic analysis for p-Gli1 and p-S6K1 correlation from the IHC staining results in human EAC tissue microarray.

(G) Statistic analysis for p-Gli1 and p-S6K1 correlation in the Gli1 positive subpopulation of human EAC tissue microarray.

See also Figure S6.

developing the antibody but not by the same nonphosphorylated peptide (Figure S6F). Moreover, using the same set of mouse colon tissues used above, we could not detect any signal of p-S6K1 and, as expected, the signal of p-Gli1 is also negative (Figure S6A, middle and right panels). Therefore, the p-Gli1 antibody is applicable for IHC. We then examined the Gli1, p-Gli1, and p-S6K1 in human EAC tissue microarray (n = 70), and the result again showed that there was a strongly positive correlation between p-S6K1 and Gli1 or p-Gli1 (Figures S6G and 6D–6F). All p-Gli1-positive tissues are also Gli1-positive, and among the Gli1-positive tissues, there is also a strong positive correlation between p-Gli1 and p-S6K1 (Figure 6G). Thus, the phosphorylation of Gli1 also exists in human EAC tumor tissues. Additionally, using human tissue microarray with multiple cancer types, we found a positive correlation between p-S6K1 and Gli1 (Figures S6H and S6I), suggesting that the regulation of Gli1 by S6K1 might be not limited to EAC and is worthwhile to be tested in multiple kinds of cancers in the future.

A Combination Therapy that Targets Both Canonical HH and mTOR/S6K1 Pathways in EAC Cells Provides Better Therapeutic Effects

Consistent with the previous reports (Berman et al., 2003; Sims-Mourtada et al., 2006), we detected the activated form of SHH protein, the amino terminal domain of SHH (SHH-N; Ng and Curran, 2011), in the EAC cell lines (Figure 7A). In addition, SHH treatment dramatically increased expression of Gli reporter (Figure S7A) and Gli1 target genes (Figure 7B). Hence, the EAC cell lines exhibit activated canonical HH pathway. Because our data have shown that in EAC cell lines mTOR/S6K1-mediated Gli1 activation is SMO-independent, we speculated that mTOR/S6K1/Gli1 should enhance the resistance of EAC cells to SMO inhibitors. As expected, the IC_{50} value of cyclopamine or GDC-0449 in BE3/S84E was much higher than that for BE3/EV, BE3/Gli1, and BE3/S84A (Figure 7C). Moreover, TNF-α treatment increased the resistance of BE3/Gli1, but not BE3/S84A, to cyclopamine or GDC-0449 (Figure 7D), suggesting that Gli1S84 phosphorylation enhances cell resistance to SMO inhibitors. Then, we examined whether a combination of inhibitors of HH and mTOR pathways would be more effective for these EAC cell lines. To avoid the killing effect of rapamycin, we first determined that 10 nM rapamycin was sufficient to inhibit the activation of S6K1 in BE3 cells but did not significantly inhibit cell viability (Figure S7B). Thus, we used 10 nM rapamycin for all subsequent experiments. We found that rapamycin treatment enhanced the efficacy of cyclopamine or GDC-0449 in the EAC cell lines (Figure 7E). Moreover, knock-down of SMO also inhibited cell viability, and rapamycin treatment further enhanced the inhibitory effect (Figure S7C). Interestingly, the effects of rapamycin on SMO inhibitors existed in BE3/Gli1 cells but not in BE3/S84E cells (Figure 7F). Therefore, the mTOR inhibitor could enhance SMO inhibitor effects in vitro through eliminating the phosphorylation of Gli1S84. For further examination of the crosstalk of mTOR and HH pathways in vivo, we performed an in vivo combination therapy using GDC-0449 and another mTOR inhibitor, RAD-001, which is widely used in combination with other antitumor drugs in clinical trials (Piguet et al., 2011; Price et al., 2010; Quek et al., 2011). We subcutaneously inoculated mice with BE3 cells and treated them with GDC-0449, RAD-001, or both and found that though

low dose RAD001 did not inhibit tumor growth, it enhanced the tumor-inhibitory effect of GDC-0449 (Figure 7G). Therefore, the combination of the inhibitors targeting the two pathways could produce better efficacy for targeted therapy.

SMO-Independent Activation of Gli1 by AKT and ERK Requires mTOR/S6K1

It has been reported that AKT and MAPK/ERK also activate HH pathway in a SMO-independent manner. Interestingly, AKT and ERK can activate the mTOR/S6K1 pathway by inhibiting the TSC1/2 complex (Lee et al., 2007a; Ma et al., 2005; Ozes et al., 2001). This prompted us to test if the mTOR/S6K1 pathway is required for the activation of Gli1 by the two kinases. Through ectopic expression of AKT or ERK, we found that Gli1 activity increased, which could be blocked by rapamycin (Figure S8). Moreover, the activation of AKT or ERK also stimulated the phosphorylation of S6K1T389 and Gli1Ser84, which was inhibited by rapamycin (Figure 8A). However, AKT and ERK lost the ability to induce Gli1 phosphorylation when S6K1 was knocked down (Figure 8B). Therefore, our results indicated that the mTOR/S6K1/Gli1 pathway might mediate the previously reported AKT and ERK-stimulated Gli1 activation (Figure 8C).

DISCUSSION

In this study, we demonstrate a SMO-independent activation of Gli1 by the mTOR/S6K1 pathway, in which activated S6K1 phosphorylates Gli1 at Ser84, resulting in its release from SuFu binding and translocation into the nucleus to activate its target genes (Figure 8C). We previously reported that the mTOR/S6K1 pathway facilitates progression from inflammation and tumorigenesis through upregulation of VEGF, as well as the subsequent angiogenesis (Lee et al., 2007a). In addition, TNF-α/mTOR can be activated by chronic inflammation in the esophagus (Yen et al., 2008). Our work herein further implies that the mTOR/S6K1 pathway might also promote EAC through the activation of Gli1. Since Gli1 is known as an oncogene (Ng and Curran, 2011), our results also provide further evidence to support the concept that chronic inflammation is an important stimulator for tumorigenesis of the esophagus (Lambert and Hainaut, 2007a, 2007b).

The canonical HH pathway is well known to have a tight negative feedback regulation, which blocks the HH ligands and inhibits SMO activation through Gli1-promoted transcription of PTCH and HH interacting protein (Katoh and Katoh, 2006). When SMO is inactivated, SuFu binds to and inhibits Gli1 function (Katoh and Katoh, 2006). Function-loss-mutation of SuFu has been shown to result in tumorigenesis due to the aberrant activation of the HH pathway (Cheng and Yue, 2008; Lee et al., 2007b). Therefore, SuFu is an important negative regulator for the HH pathway and acts as a tumor suppressor. In this study, we found that the phosphorylation of Gli1 by S6K1 blocked the interaction between SuFu and Gli1, allowing Gli1 to translocate into the nucleus to activate transcription of HH target genes. Thus, in contrast to the canonical HH pathway, SMO inhibitors do not seem to affect S6K1-mediated Gli1 activation, suggesting that the S6K1-mediated release of SuFu from Gli1 occurs independently of SMO. In fact, SMO inhibitors, such as cyclopamine and GDC-0449, had little effects on the mTOR/S6K1-mediated Gli1 activation. These findings suggest that the mTOR/S6K1 pathway can act as a positive modulator to amplify and fuel Gli1 activation to promote tumorigenesis and disease progression.

The HH pathway has been considered as a therapeutic target for GI cancers, including esophageal cancers (Lee et al., 2009; Wiedmann and Caca, 2005). Several SMO inhibitors, including GDC-0449, are currently being tested in clinical trials, which are either structurally derived from or functionally similar to cyclopamine (Scales and de Sauvage, 2009; Stanton and Peng, 2010). Our data showed that the administration of GDC-0449 indeed decreased the EAC tumor size, supporting that GDC-0449 also could be used for treating EAC (Figure 7G). In this study, however, we disclose a SMO-independent activation of Gli1 by the mTOR/S6K1 pathway, which cannot be inhibited by SMO inhibitors but is sensitive to inhibitors of the mTOR pathways. Cotreatment with mTOR/S6K1 and SMO inhibitors, RAD001 and GDC-0449, indeed showed better inhibitory effects on tumor growth in vivo than did single drug treatment. Therefore, our results strongly suggest that a combination of inhibitors targeting the two pathways may be a more effective strategy to treat EAC.

In addition, through the immunostaining analysis of human EAC tissues, we found that in about 40% (28/70) of patients, all of the p-Gli1, Gli1, and p-S6K1 were positive, suggesting that these patients may bear both canonical HH pathway and mTOR/S6K1-mediated SMO-independent Gli1 activation. Based on the current study, we would predict that this population of patients may not have full response to GDC-0449 treatment alone but could benefit from the proposed cotreatment of inhibitors targeting both the mTOR and HH pathways. Therefore, a preselection procedure might be required for the patients before receiving the SMO inhibitors to determine whether the cotreatment strategy should be applied. It is worthwhile to mention that many inhibitors targeting these two pathways are being tested in clinical trials, such as GDC-0449 and IPI-926, targeting the HH pathway (Stanton and Peng, 2010), and RAD001 and AP23573, targeting the mTOR pathway (Konings et al., 2009). Thus, exploring a vast array of possible therapeutic combinations will be useful to simultaneously target these pathways.

Although SMO inhibitors are known to inhibit several types of cancer and have shown hopeful tumor-inhibitory effects, the development of resistance due to the constitutive activation mutation of SMO or overactivation of PI3K/AKT pathway has been reported (Metcalfe and de Sauvage, 2011). Buonamici et al. further showed that the resistance of medulloblastoma to SMO inhibitors could be decreased through a combination of SMO and PI3K/AKT inhibitors (Buonamici et al., 2010). Interestingly, PI3K/AKT and RAS/MEK/ERK have been also found to activate Gli1 in a SMO-independent manner (Katoh and Katoh, 2009b; Seto et al., 2009; Stecca et al., 2007), though the mechanisms are not well understood. Because AKT and ERK can activate the mTOR/S6K1 pathway (Ma et al., 2005; Ozes et al., 2001) and activation of Gli1 by AKT or ERK requires S6K1 (Figure 8B), our finding that S6K1 phosphorylates Gli1 and enhances its function provides a molecular mechanism not only for mTOR/S6K1-mediated but also AKT or ERK-induced SMO-independent Gli1 activation (Figure 8C). Thus, our results also provide a potential explanation for the resistance of tumor cells to SMO inhibitors. Similarly, our study offers a rationale for combining

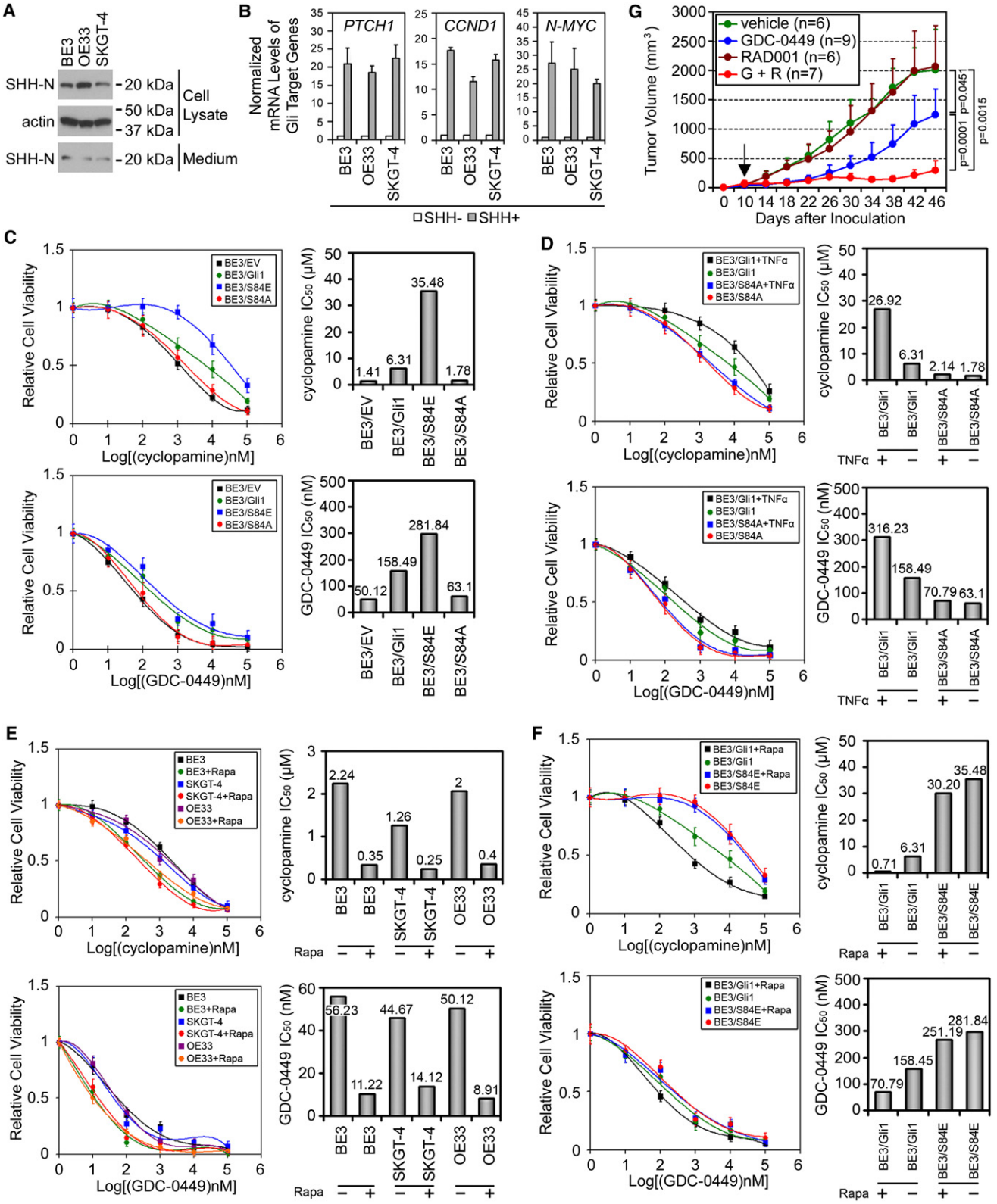

Figure 7. Effects of mTOR and/or HH Pathway Inhibitors on EAC Cells

(A) The expression of activated SHH (SHH-N) in EAC cell lines and the cell culture medium.

(B) The mRNA levels of Gli1 target genes in EAC cell lines with or without SHH treatment (1 μg/ml) induces the upregulation of. The mRNA levels of Gli1 target genes are normalized to *ACTIN*. Error bars represent SD (n = 3).

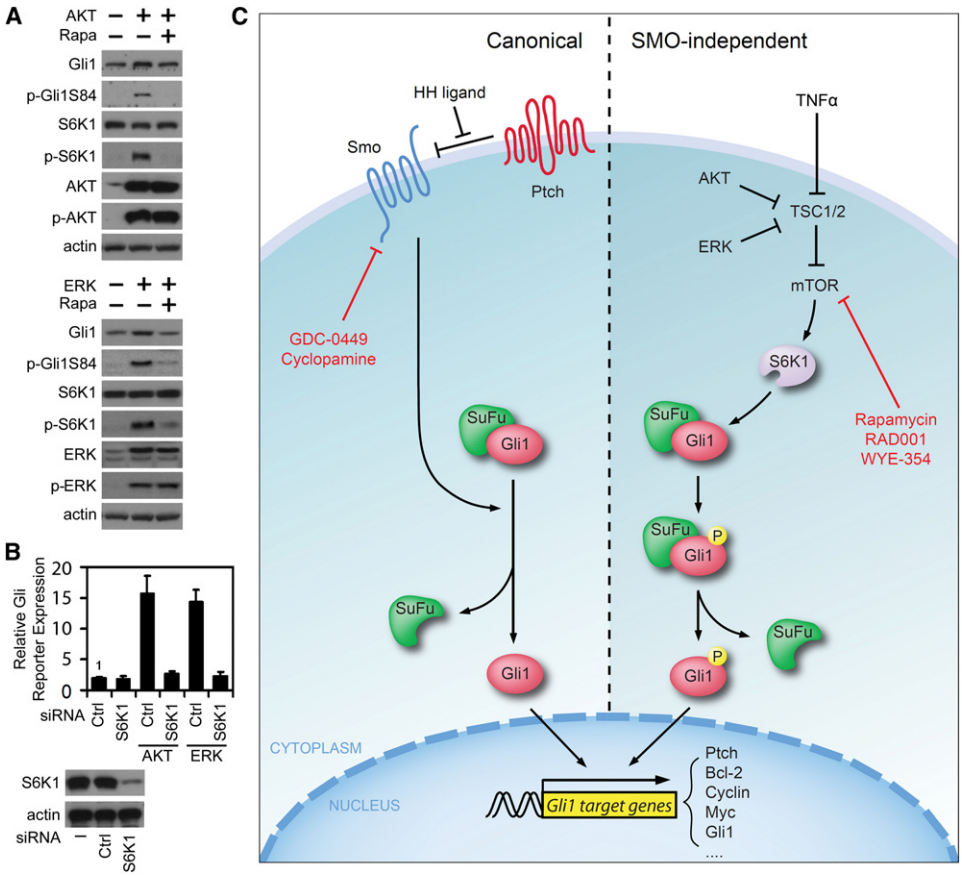

Figure 8. AKT and ERK Can Activate Gli1 through mTOR/S6K1 Pathway

(A) The regulation of S6K1 and Gli1 by ectopically expressed AKT or ERK in HeLa cells with or without rapamycin (50 nM).

(B) The influence of S6K1 knock-down on the AKT or ERK-stimulated HH pathway in HeLa cells. Error bars represent SD (n = 3).

(C) Schematic diagram for the canonical HH pathway stimulated by HH ligands and SMO-independent Gli1 activation stimulated by the mTOR/S6K1 pathway.

See also Figure S8.

SMO with mTOR/S6K1 inhibitors to increase the effectiveness for treating EAC.

Taken together, our current study identifies Gli1 as a substrate for S6K1 and establishes a crosstalk between the mTOR/S6K1 and HH pathways, providing a mechanism for SMO-independent Gli1 activation. Our data also suggest that the combination of the inhibitors to these two pathways has a more potent inhibitory effect on the EAC cells than single agent alone. Moreover, we also found the correlation between p-S6K1 and Gli1 of multiple cancer types using tissue microarray, indicating that the combined targeted therapy, targeting both the mTOR/S6K1 and HH pathways, may be effective for treatment of EAC, as well as other cancers.

EXPERIMENTAL PROCEDURES

Human Tissues

Human EAC specimens for immunohistochemistry were obtained retrospectively from patients undergoing complete esophageal surgical resection, as primary treatment, at MD Anderson Cancer Center (MDACC) between January 1986 and December 1997. The specimen collection was conducted in accordance with the protocols approved by the Institutional Review Board at MD Anderson Cancer Center, and written informed consent was obtained from

(C) IC_{50} of cyclopamine (top two panels) or GDC-0449 (bottom two panels) for the Gli1 stable clones. Error bars represent SD (n = 4).

(D) IC_{50} of cyclopamine (top two panels) or GDC-0449 (bottom two panels) for the Gli1 stable clones with existence of TNF-α (5 ng/ml). Error bars represent SD (n = 4).

(E) IC_{50} of cyclopamine (top two panels) or GDC-0449 (bottom two panels) for EAC cells pretreated with rapamycin (Rapa, 10 nM). Error bars represent SD (n = 4).

(F) IC_{50} of cyclopamine (top two panels) or GDC-0449 (bottom two panels) for the Gli1 stable clones with rapamycin (Rapa, 50 nM) treatment. Error bars represent SD (n = 4).

(G) In vivo combination therapy for subcutaneously inoculated tumors from BE3 cells using GDC-0449 (50 mg/kg) or RAD001 (10 mg/kg). BE3 cells 1×10^6 were subcutaneously injected into the right flank of nude mice, and the tumor cells were allowed to grow for 10 days (the arrow) before initiation of drug treatment. The vehicle, GDC-0449, RAD001, or combination of GDC-0449 and RAD001, was orally administrated, qd. The tumor volume measured and calculated using the formula $l \times w^2$, where l is the longest diameter and w is the shortest diameter. Error bars represent SD (n = 5).

See also Figure S7.

patients in all cases at time of enrollment. The multiple tissue microarrays were purchased from US Biomax, Inc. (BC00112 and MTU241; Rockville, MD, USA).

Immunoprecipitation, Immunoblotting, and In Vitro Kinase Assays

Immunoprecipitation and immunoblotting were performed as previously described (Lee et al., 2007a). For in vitro kinase assay, the BL21 competent cells were transformed with pGEX-6P-1, pGEX-6P-1-S6, pGEX-6P-1-Gli1F1, or pGEX-6P-1-Gli1F2 vectors. After overnight growth, the cells were lysed, and the target proteins were purified using the GST antibody crosslinked agarose beads (Thermo Scientific, Hudson, NH, USA) in accordance with the manufacturer's instruction. In addition, 90% confluent BE3 cells were transfected with HA-S6K1, HA-S6K1T389E, HA-S6K1T389A, or HA-S6K1K100R, and 24 hr after transfection, the cells were lysed and immunoprecipitated with anti-HA antibody. Purified GST protein or GST fusion proteins were incubated with purified HA-S6K1 or HA-S6K1 mutants in the presence of 50 mM ATP in a kinase buffer for 30 min at 30°C. Reaction products were subjected to SDS-PAGE (sodium dodecyl sulfate polyacrylamide gel electrophoresis (SDS-PAGE) and then blotted with phosphor-Thr/Ser antibody.

IC_{50} Evaluation for Cyclopamine and GDC-0449

Cells were seeded in 96-well plates at the density of 5,000 cells/well. After overnight growth, the cells were exposed to increasing concentrations, ranging from 1 nM to 100 μM for cyclopamine or GDC-0449, with or without 10 nM rapamycin, for 48 hr. The concentrations required to inhibit cell growth by 50% (IC_{50}) were calculated from survival curves.

Rat Model of BE and EAC

The rat model was established as previously described (Yen et al., 2008). The excised esophageal tissues from normal esophagus, BE, or EAC were fixed in 10% buffered formalin for 24 hr and then transferred to 80% ethanol. The tissue was longitudinally divided into slices for immunohistochemistry staining.

Tumorigenicity Assay and Combination Therapy In Vivo

All animal experiments were approved by the Institutional Animal Care and Use Committee (IACUC) at MD Anderson Cancer Center. Nude female mice were housed under standard conditions. For tumorigenicity assay, 1×10^5 BE3 stable cells were subcutaneously injected in right flank. The resulting tumors were measured with calipers weekly, and tumor volume was determined using the formula $l \times w^2$, where l is the longest diameter and w is the shortest diameter. For combination therapy, 1×10^6 BE3 cells were subcutaneously injected in right flanks of nude mice and allowed to grow for 10 days before drug treatment. GDC-0449 was formulated in MCT (0.5% methylcellulose and 0.5% Tween 80) and RAD001 in water. GDC-0449 (50 mg/kg) and RAD001 (10 mg/kg) were dosed qd (quaque die (qd) by oral gavage. The tumors were measured with calipers every 4 days. Data were presented as tumor volume (mean ± SD). Statistical analysis was done using the Student's t test by the program SPSS for Windows.

Statistical Analyses

Statistical analyses were performed with the Student's t test, Spearman rank correlation test, or Fisher's exact test as indicated. A p value of <0.05 was considered statistically significant. All data analyses were performed using the program SPSS for Windows.

All other experimental procedures are described in the Supplemental Experimental Procedures.

SUPPLEMENTAL INFORMATION

Supplemental Information includes eight figures and Supplemental Experimental Procedures and can be found with this article online at doi:10.1016/j.ccr.2011.12.028.

ACKNOWLEDGMENTS

We thank Dr. Anthony E. Oro for providing the Gli1-expressing plasmid; Rune Toftgård for SuFu-expressing plasmid; and Dr. Hiroshi Sasaki for Gli1-reporter plasmids. We thank Jer-Yen Yang for insightful discussion and Su Zhang, Jian-Guang Shi, Zhen-Bo Han, and Jin-Fong Lee for technical assistance. This work was supported by the National Institutes of Health (CA109311and CA099031 to M.-C.H and CCSG Core Grant CA16672); the Kadoorie Charitable Foundation; the Center for Biological Pathway at the University of Texas, MD Anderson Cancer Center; Susan G. Komen (SAC110016 to M.-C.H), the Sister Institution Fund of China Medical University and Hospital and the University of Texas, MD Anderson Cancer Center; Department of Health Cancer Research Center of Excellence (DOH101-TD-C-111-005, Taiwan; NSC100-2321-B-039-002, Taiwan; NSC99-2632-B-039-001-MY3, Taiwan); the Dallas, Park, Sultan, Smith, and Cantu Family funds (to J.A.); the Reivercreek and Schecter Private foundations (to J.A.); Kevin and Frazier funds (to J.A.); National Cancer Institute (CA142072, CA127672, and CA129906 to J.A.); and the University of Texas, MD Anderson Cancer Center Multidisciplinary Research Program Funding.

Received: July 8, 2011
Revised: October 13, 2011
Accepted: December 30, 2011
Published: March 19, 2012

REFERENCES

Berman, D.M., Karhadkar, S.S., Maitra, A., Montes De Oca, R., Gerstenblith, M.R., Briggs, K., Parker, A.R., Shimada, Y., Eshleman, J.R., Watkins, D.N., and Beachy, P.A. (2003). Widespread requirement for Hedgehog ligand stimulation in growth of digestive tract tumours. Nature *425*, 846–851.

Boonstra, J.J., van Marion, R., Beer, D.G., Lin, L., Chaves, P., Ribeiro, C., Pereira, A.D., Roque, L., Darnton, S.J., Altorki, N.K., et al. (2010). Verification and unmasking of widely used human esophageal adenocarcinoma cell lines. J. Natl. Cancer Inst. *102*, 271–274.

Brown, E.J., Beal, P.A., Keith, C.T., Chen, J., Shin, T.B., and Schreiber, S.L. (1995). Control of p70 s6 kinase by kinase activity of FRAP in vivo. Nature *377*, 441–446.

Buonamici, S., Williams, J., Morrissey, M., Wang, A., Guo, R., Vattay, A., Hsiao, K., Yuan, J., Green, J., Ospina, B., et al. (2010). Interfering with resistance to smoothened antagonists by inhibition of the PI3K pathway in medulloblastoma. Sci Transl Med *2*, 51ra70.

Cheng, S.Y., and Yue, S. (2008). Role and regulation of human tumor suppressor SUFU in Hedgehog signaling. Adv. Cancer Res. *101*, 29–43.

Di Marcotullio, L., Ferretti, E., Greco, A., De Smaele, E., Po, A., Sico, M.A., Alimandi, M., Giannini, G., Maroder, M., Screpanti, I., and Gulino, A. (2006). Numb is a suppressor of Hedgehog signalling and targets Gli1 for Itch-dependent ubiquitination. Nat. Cell Biol. *8*, 1415–1423.

Eksteen, J.A., Scott, P.A., Perry, I., and Jankowski, J.A. (2001). Inflammation promotes Barrett's metaplasia and cancer: a unique role for TNFalpha. Eur. J. Cancer Prev. *10*, 163–166.

Fukaya, M., Isohata, N., Ohta, H., Aoyagi, K., Ochiya, T., Saeki, N., Yanagihara, K., Nakanishi, Y., Taniguchi, H., Sakamoto, H., et al. (2006). Hedgehog signal activation in gastric pit cell and in diffuse-type gastric cancer. Gastroenterology *131*, 14–29.

Guertin, D.A., and Sabatini, D.M. (2007). Defining the role of mTOR in cancer. Cancer Cell *12*, 9–22.

Hildebrandt, M.A., Yang, H., Hung, M.C., Izzo, J.G., Huang, M., Lin, J., Ajani, J.A., and Wu, X. (2009). Genetic variations in the PI3K/PTEN/AKT/mTOR pathway are associated with clinical outcomes in esophageal cancer patients treated with chemoradiotherapy. J. Clin. Oncol. *27*, 857–871.

Holz, M.K., Ballif, B.A., Gygi, S.P., and Blenis, J. (2005). mTOR and S6K1 mediate assembly of the translation preinitiation complex through dynamic protein interchange and ordered phosphorylation events. Cell *123*, 569–580.

Hongo, M., Nagasaki, Y., and Shoji, T. (2009). Epidemiology of esophageal cancer: Orient to Occident. Effects of chronology, geography and ethnicity. J. Gastroenterol. Hepatol. *24*, 729–735.

Ingham, P.W., and McMahon, A.P. (2001). Hedgehog signaling in animal development: paradigms and principles. Genes Dev. *15*, 3059–3087.

Jemal, A., Siegel, R., Ward, E., Hao, Y., Xu, J., and Thun, M.J. (2009). Cancer statistics, 2009. CA Cancer J. Clin. *59*, 225–249.

Jenkins, D. (2009). Hedgehog signalling: emerging evidence for non-canonical pathways. Cell. Signal. *21*, 1023–1034.

Jiang, J., and Hui, C.C. (2008). Hedgehog signaling in development and cancer. Dev. Cell *15*, 801–812.

Katoh, Y., and Katoh, M. (2006). Hedgehog signaling pathway and gastrointestinal stem cell signaling network (review). Int. J. Mol. Med. *18*, 1019–1023.

Katoh, Y., and Katoh, M. (2009a). Hedgehog target genes: mechanisms of carcinogenesis induced by aberrant hedgehog signaling activation. Curr. Mol. Med. *9*, 873–886.

Katoh, Y., and Katoh, M. (2009b). Integrative genomic analyses on GLI1: positive regulation of GLI1 by Hedgehog-GLI, TGFbeta-Smads, and RTK-PI3K-AKT signals, and negative regulation of GLI1 by Notch-CSL-HES/HEY, and GPCR-Gs-PKA signals. Int. J. Oncol. *35*, 187–192.

Kolterud, A., Grosse, A.S., Zacharias, W.J., Walton, K.D., Kretovich, K.E., Madison, B.B., Waghray, M., Ferris, J.E., Hu, C., Merchant, J.L., et al. (2009). Paracrine Hedgehog signaling in stomach and intestine: new roles for hedgehog in gastrointestinal patterning. Gastroenterology *137*, 618–628.

Konings, I.R., Verweij, J., Wiemer, E.A., and Sleijfer, S. (2009). The applicability of mTOR inhibition in solid tumors. Curr. Cancer Drug Targets *9*, 439–450.

Lambert, R., and Hainaut, P. (2007a). Esophageal cancer: cases and causes (part I). Endoscopy *39*, 550–555.

Lambert, R., and Hainaut, P. (2007b). Esophageal cancer: the precursors (part II). Endoscopy *39*, 659–664.

Lee, D.F., Kuo, H.P., Chen, C.T., Hsu, J.M., Chou, C.K., Wei, Y., Sun, H.L., Li, L.Y., Ping, B., Huang, W.C., et al. (2007a). IKK beta suppression of TSC1 links inflammation and tumor angiogenesis via the mTOR pathway. Cell *130*, 440–455.

Lee, D.Y., Deng, Z., Wang, C.H., and Yang, B.B. (2007b). MicroRNA-378 promotes cell survival, tumor growth, and angiogenesis by targeting SuFu and Fus-1 expression. Proc. Natl. Acad. Sci. USA *104*, 20350–20355.

Lee, W., Patel, J.H., and Lockhart, A.C. (2009). Novel targets in esophageal and gastric cancer: beyond antiangiogenesis. Expert Opin. Investig. Drugs *18*, 1351–1364.

Ma, L., Chen, Z., Erdjument-Bromage, H., Tempst, P., and Pandolfi, P.P. (2005). Phosphorylation and functional inactivation of TSC2 by Erk implications for tuberous sclerosis and cancer pathogenesis. Cell *121*, 179–193.

Metcalfe, C., and de Sauvage, F.J. (2011). Hedgehog fights back: mechanisms of acquired resistance against Smoothened antagonists. Cancer Res. *71*, 5057–5061.

Ng, J.M., and Curran, T. (2011). The Hedgehog's tale: developing strategies for targeting cancer. Nat. Rev. Cancer *11*, 493–501.

Nolan-Stevaux, O., Lau, J., Truitt, M.L., Chu, G.C., Hebrok, M., Fernández-Zapico, M.E., and Hanahan, D. (2009). GLI1 is regulated through Smoothened-independent mechanisms in neoplastic pancreatic ducts and mediates PDAC cell survival and transformation. Genes Dev. *23*, 24–36.

Ozes, O.N., Akca, H., Mayo, L.D., Gustin, J.A., Maehama, T., Dixon, J.E., and Donner, D.B. (2001). A phosphatidylinositol 3-kinase/Akt/mTOR pathway mediates and PTEN antagonizes tumor necrosis factor inhibition of insulin signaling through insulin receptor substrate-1. Proc. Natl. Acad. Sci. USA *98*, 4640–4645.

Piguet, A.C., Saar, B., Hlushchuk, R., St-Pierre, M.V., McSheehy, P.M., Radojevic, V., Afthinos, M., Terracciano, L., Djonov, V., and Dufour, J.F. (2011). Everolimus augments the effects of sorafenib in a syngeneic orthotopic model of hepatocellular carcinoma. Mol. Cancer Ther. *10*, 1007–1017.

Price, K.A., Azzoli, C.G., Krug, L.M., Pietanza, M.C., Rizvi, N.A., Pao, W., Kris, M.G., Riely, G.J., Heelan, R.T., Arcila, M.E., and Miller, V.A. (2010). Phase II trial of gefitinib and everolimus in advanced non-small cell lung cancer. J. Thorac. Oncol. *5*, 1623–1629.

Quek, R., Wang, Q., Morgan, J.A., Shapiro, G.I., Butrynski, J.E., Ramaiya, N., Huftalen, T., Jederlinic, N., Manola, J., Wagner, A.J., et al. (2011). Combination mTOR and IGF-1R inhibition: phase I trial of everolimus and figitumumab in patients with advanced sarcomas and other solid tumors. Clin. Cancer Res. *17*, 871–879.

Richard, D.J., Verheijen, J.C., and Zask, A. (2010). Recent advances in the development of selective, ATP-competitive inhibitors of mTOR. Curr. Opin. Drug Discov. Devel. *13*, 428–440.

Sasaki, H., Hui, C., Nakafuku, M., and Kondoh, H. (1997). A binding site for Gli proteins is essential for HNF-3beta floor plate enhancer activity in transgenics and can respond to Shh in vitro. Development *124*, 1313–1322.

Scales, S.J., and de Sauvage, F.J. (2009). Mechanisms of Hedgehog pathway activation in cancer and implications for therapy. Trends Pharmacol. Sci. *30*, 303–312.

Seto, M., Ohta, M., Asaoka, Y., Ikenoue, T., Tada, M., Miyabayashi, K., Mohri, D., Tanaka, Y., Ijichi, H., Tateishi, K., et al. (2009). Regulation of the hedgehog signaling by the mitogen-activated protein kinase cascade in gastric cancer. Mol. Carcinog. *48*, 703–712.

Sims-Mourtada, J., Izzo, J.G., Apisarnthanarax, S., Wu, T.T., Malhotra, U., Luthra, R., Liao, Z., Komaki, R., van der Kogel, A., Ajani, J., and Chao, K.S. (2006). Hedgehog: an attribute to tumor regrowth after chemoradiotherapy and a target to improve radiation response. Clin. Cancer Res. *12*, 6565–6572.

Stanton, B.Z., and Peng, L.F. (2010). Small-molecule modulators of the Sonic Hedgehog signaling pathway. Mol. Biosyst. *6*, 44–54.

Stecca, B., Mas, C., Clement, V., Zbinden, M., Correa, R., Piguet, V., Beermann, F., and Ruiz I Altaba, A. (2007). Melanomas require HEDGEHOG-GLI signaling regulated by interactions between GLI1 and the RAS-MEK/AKT pathways. Proc. Natl. Acad. Sci. USA *104*, 5895–5900.

Wiedmann, M.W., and Caca, K. (2005). Molecularly targeted therapy for gastrointestinal cancer. Curr. Cancer Drug Targets *5*, 171–193.

Yen, C.J., Izzo, J.G., Lee, D.F., Guha, S., Wei, Y., Wu, T.T., Chen, C.T., Kuo, H.P., Hsu, J.M., Sun, H.L., et al. (2008). Bile acid exposure up-regulates tuberous sclerosis complex 1/mammalian target of rapamycin pathway in Barrett's-associated esophageal adenocarcinoma. Cancer Res. *68*, 2632–2640.

Zoncu, R., Efeyan, A., and Sabatini, D.M. (2011). mTOR: from growth signal integration to cancer, diabetes and ageing. Nat. Rev. Mol. Cell Biol. *12*, 21–35.